

Quantum criticality in NdFe₂Ga₈ under magnetic field


Cuixiang Wang^{1,2,3}, Xingyu Wang^{1,3}, Le Wang¹, Meng Yang^{1,3}, Youting Song¹, Zhenyu Mi^{1,4}, Gang Li^{1,4}, Youguo Shi^{1,2,4,*}, Shiliang Li^{1,3,4,†} and Yi-feng Yang^{1,3,4,‡}

¹Beijing National Laboratory for Condensed Matter Physics, Institute of Physics, Chinese Academy of Sciences, Beijing 100190, China

²Center of Materials Science and Optoelectronics Engineering, University of Chinese Academy of Sciences, Beijing 100049, China

³School of Physical Sciences, University of Chinese Academy of Sciences, Beijing 100190, China

⁴Songshan Lake Materials Laboratory, Dongguan, Guangdong 523808, China

 (Received 28 August 2020; revised 29 October 2020; accepted 10 December 2020; published 7 January 2021)

We studied the magnetism in NdFe₂Ga₈ by magnetic susceptibility, specific heat, and resistivity measurements, which show Nd³⁺ ions forming one-dimensional chains along the *c* axis. At zero field, two magnetic transitions are found at about 15 and 11 K. For field vertical to the *c* axis, no significant effects on the magnetic orders are found. On the other hand, the two transitions are merged together at about 4 T for field parallel to the *c* axis and completely suppressed at about 7 T. The suppression of the magnetic order results in quantum critical behaviors of the conventional three-dimensional spin-density-wave type, such as $\rho \sim T^{1.5}$ and $C/T \sim T^{-0.5}$. However, the temperature dependence of the resistivity is replaced by a $T^{0.5}$ behavior at very low temperatures for field larger than 3 T, which is attributed to the field-induced ferromagnetic moment. Our results suggest that there may be couplings between the antiferromagnetic quantum critical fluctuations and the field-induced ferromagnetic fluctuations.

DOI: [10.1103/PhysRevB.103.035107](https://doi.org/10.1103/PhysRevB.103.035107)

I. INTRODUCTION

Heavy-fermion materials provide an excellent platform for studying quantum criticality, which results from a quantum critical point (QCP) at zero temperature that gives rise to non-Fermi-liquid (NFL) behaviors. Because both itinerant and local degrees of freedom play crucial roles in determining their ground states, the QCPs in heavy-fermion materials show rich properties [1–3]. For example, in some heavy-fermion compounds [4–11], the magnetic phase can be understood as the itinerant spin density wave (SDW), where the electrons forming the Fermi surface are responsible for both the magnetic order and the associated QCP. This type of QCP is called the conventional QCP, which can be described by conventional SDW theories [1,12]. On the other hand, the spin and charge of the heavy quasiparticles may be separated, and the Fermi surface thus changes simultaneously at the QCP [1–3]. This type of QCP is called the unconventional QCP. Pursuing different types of QCPs has always been one of the major interests in studying heavy-fermion materials.

Recently, there has been increasing interest in the heavy-fermion physics in the so-called 1-2-8 systems [13–26]. Here “1-2-8” represents LM_2T_8 , where *L* is the Lanthanum (La, Nd, Ce, etc.), *M* is the transition metal (Fe, Co, Ru, etc.), and *T* indicates the triels (boron group, Al, Ga, In). They have an orthorhombic structure with the space group *Pbam* (No. 55), where the lanthanum ions form one-dimensional (1D) chains, so the magnetism of the 4*f* electrons is expected to

show 1D characteristics. For Pr- and Nd-based 1-2-8 compounds, most of them show long-range magnetic ordering at low temperatures [20–25]. For Ce-based 1-2-8 compounds, the spin system typically shows no magnetic ordering except for CePd₂Al₈ [13–20]. It should be noted that the magnetic ordering in these materials is found to solely come from the 4*f* electrons, not the 3*d* electrons, although the latter may form clusters at low temperatures [14]. Therefore, the 1-2-8 systems provide an interesting platform to study the quantum criticality from heavy 4*f* electrons. It is thus particularly interesting to see that the CeCo₂Ga₈ system shows typical QCP behaviors, such as the divergence of magnetic susceptibility and specific heat ($\chi \sim -\ln T$, $C/T \sim -\ln T$), and NFL behavior of the resistivity ($\rho \sim T$) [18,19]. This naturally raises the question of whether a QCP can exist in other 1-2-8 systems.

In this work, we systematically study the magnetism in NdFe₂Ga₈ under the magnetic field. At zero field, two magnetic transitions are found at about 15 and 11 K, respectively. While these two transitions are hardly affected by the field within the *ab* plane, a 7-T magnetic field along the *c* axis can completely suppress the magnetic orders and may result in a QCP. At relatively high temperatures, it is, indeed, found that $C/T \propto T^{-1/2}$ and $\rho \propto T^{3/2}$, which suggest that the quantum criticality in NdFe₂Ga₈ belongs to the class of the three-dimensional (3D) SDW. However, magnetic hysteresis behaviors are found in the ordered state and persist even above 7 T at low temperatures, which precludes the actual existence of a QCP. Moreover, at very low temperatures, C/T becomes temperature independent and $\rho \propto T^{1/2}$ around 7 T, which may be associated with the field-induced ferromagnetic (FM) moment.

*ygshi@iphy.ac.cn

†slli@iphy.ac.cn

‡yifeng@iphy.ac.cn

II. EXPERIMENTS

Single crystals of NdFe_2Ga_8 and LaFe_2Ga_8 were grown by the self-flux method. The mixture of the starting materials with Nd (99.99%) or La(99.99%), Fe (99.95%), and Ga (99.9999%) with a molar ratio of 1:2:20 was put in an alumina crucible and then sealed in a quartz tube under vacuum. After heating the mixture at 1150°C for 24 hours, the temperature was decreased to 750°C at a rate of 2°C per hour. Crystals were obtained after immediately centrifuging to remove Ga flux. The crystals have the shape of a hexagonal prism with a height of several millimeters. The hexagonal base is typically just about 0.1–0.2 mm in diameter but occasionally can be about 1 mm. The chemical components were analyzed by energy dispersive x-ray spectroscopy and inductively coupled plasma measurements. The crystal structure was measured by both powder and single-crystal x-ray diffractometers (XRDs). The magnetic susceptibility was measured using a magnetic property measurement system (Quantum Design). The measurements of resistivity and specific heat were carried out in a physical property measurement system (Quantum Design).

III. RESULTS AND DISCUSSION

Figure 1(a) shows the crystal structure of NdFe_2Ga_8 that was previously reported for the polycrystalline sample [13]. Figure 1(b) gives the powder diffraction pattern of ground samples, which can be refined very well with the above struc-

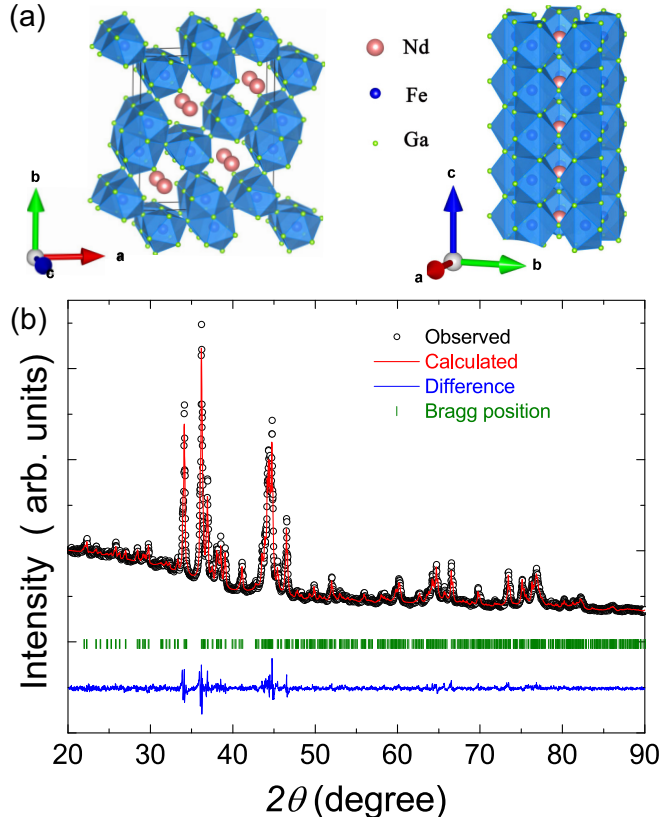


FIG. 1. (a) Crystal structure of NdFe_2Ga_8 . The black lines represent the unit cell. (b) XRD results of ground NdFe_2Ga_8 with $R_p = 2.31\%$, $R_{wp} = 3.21\%$, and $\chi = 1.36$.

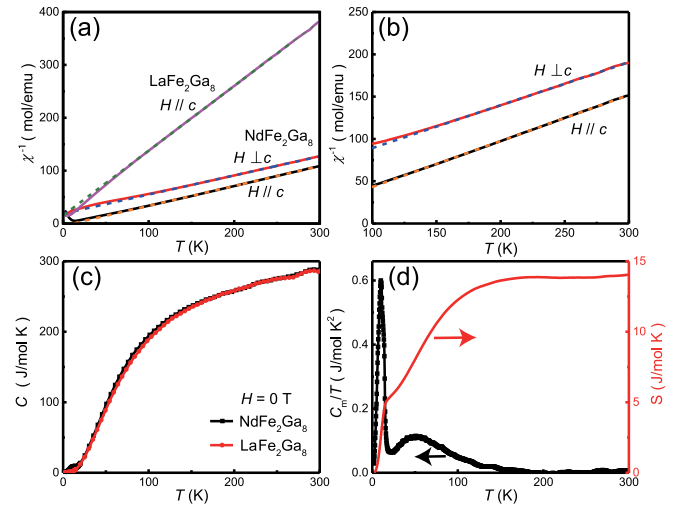


FIG. 2. (a) and (b) Temperature dependence of the inverse magnetic susceptibility for NdFe_2Ga_8 and LaFe_2Ga_8 , respectively. The dashed lines are results fitted by the Curie-Weiss function as described in the main text. (c) The temperature dependence of specific heats of NdFe_2Ga_8 and LaFe_2Ga_8 at zero field. (d) The temperature dependence of the magnetic specific heat from Nd moments and the corresponding entropy.

ture. The results from the single-crystal XRD are the same. As Nd ions form 1D chains along the *c* axis, the magnetism is expected to show strong anisotropic properties, which have, indeed, been observed, as shown below.

Figure 2(a) shows the temperature dependence of the inverse magnetic susceptibility for NdFe_2Ga_8 , which shows magnetic transitions at low temperature that will be discussed in detail later. The high-temperature data can be fitted linearly, which comes from the Curie-Weiss function $\chi = C/(T - \theta)$, where C and θ are the Curie constant and Weiss temperature, respectively. For both field directions, the effective moment μ_{eff} of NdFe_2Ga_8 determined from the Curie constant is about $4.65\mu_B$, which is larger than that of the free Nd^{3+} ion ($3.62\mu_B$), suggesting contributions from both Nd and Fe moments. As a comparison, the Curie-Weiss fit on the high-temperature data of LaFe_2Ga_8 shown in Fig. 2(a) gives $\mu_{\text{eff}}^{\text{Fe}} = 1.81\mu_B$. We can derive $\mu_{\text{eff}}^{\text{Nd}}$ from the difference of the magnetic susceptibility $\Delta\chi$ between these two samples, as shown in Fig. 2(b), which gives $\mu_{\text{eff}}^{\text{Nd}}$ of about $3.9\mu_B$, much closer to the value of the free Nd^{3+} ion. The Weiss temperatures are 20.6 and -75.8 K for magnetic field parallel and vertical to the *c* axis, respectively, which suggests that the dominating interactions along the *c* axis and within the *ab* plane are FM and antiferromagnetic (AFM), respectively. It is clear that although the Nd^{3+} ions show 1D chain structure, the exchange energy vertical to the chains is actually much larger than that along the chains.

Figure 2(c) shows the temperature dependence of the specific heat for both NdFe_2Ga_8 and LaFe_2Ga_8 at zero field. At high temperatures (>200 K), the data overlap with each other, confirming that the latter can be used as a background to subtract the magnetic specific heat of the former. The difference is shown in Fig. 2(e), where the entropy released just above the magnetic transition (~ 15 K) is close to $R \ln 2$. As

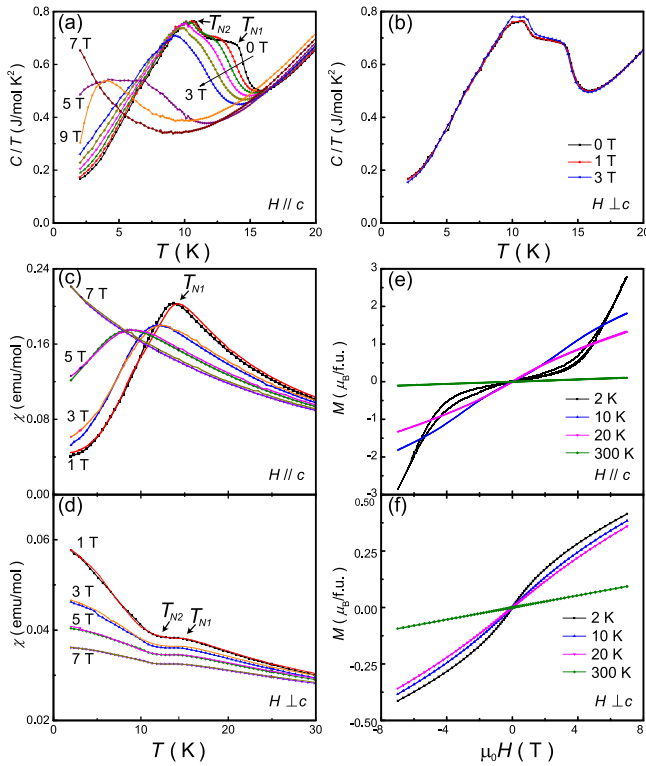


FIG. 3. (a) and (b) Temperature dependence of the specific heat C/T of NdFe_2Ga_8 for $H//c$ and $H\perp c$, respectively. All the data are from NdFe_2Ga_8 from now on. Two magnetic transitions at 0 T are labeled as T_{N1} and T_{N2} . (c) and (d) Temperature dependence of magnetic susceptibility $\chi = M/H$ for $H//c$ and $H\perp c$, respectively. Only T_{N1} is visible for $H//c$. The symbols and lines are results of the zero-field-cooling and field-cooling measurements, respectively. (e) and (f) Magnetic hysteresis curves for $H//c$ and $H\perp c$, respectively.

NdFe_2Ga_8 adopts the YbCo_2Al_8 -type orthorhombic structure with space group $Pbam$ (No. 55), where Nd^{3+} ions are located on a site with only mirror symmetry, the Nd $4f$ orbitals are completely split by the crystal field, and one expects five Kramers doublets. The entropy released below T_{N1} suggests that the ground state is a doublet. The whole entropy below room temperature is about 70% of $R \ln 10$ for $J = 9/2$. These results suggest that the low-temperature magnetic orders are mainly associated with Nd^{3+} moments.

The low-temperature magnetic properties show strong anisotropic behaviors, as shown in Fig. 3. Zero-field specific-heat data reveal two magnetic transitions at about 15 and 11 K, labeled T_{N1} and T_{N2} , respectively [Fig. 3(a)]. For $H//c$, both transitions are quickly suppressed with increasing field and merge into one above 3 T. On the other hand, little effect is observed for $H\perp c$, as shown in Fig. 3(b). It is interesting to note that when the magnetic order is suppressed at about 7 T for $H//c$, a quick upturn of C/T appears at low temperatures, as shown in Fig. 3(a).

Figures 3(c) and 3(d) show the temperature dependence of magnetic susceptibilities for H parallel and vertical to the c axis, respectively. Consistent with the specific-heat data, the magnetic order is significantly affected only for $H//c$. We note that whereas there are indications of two transitions

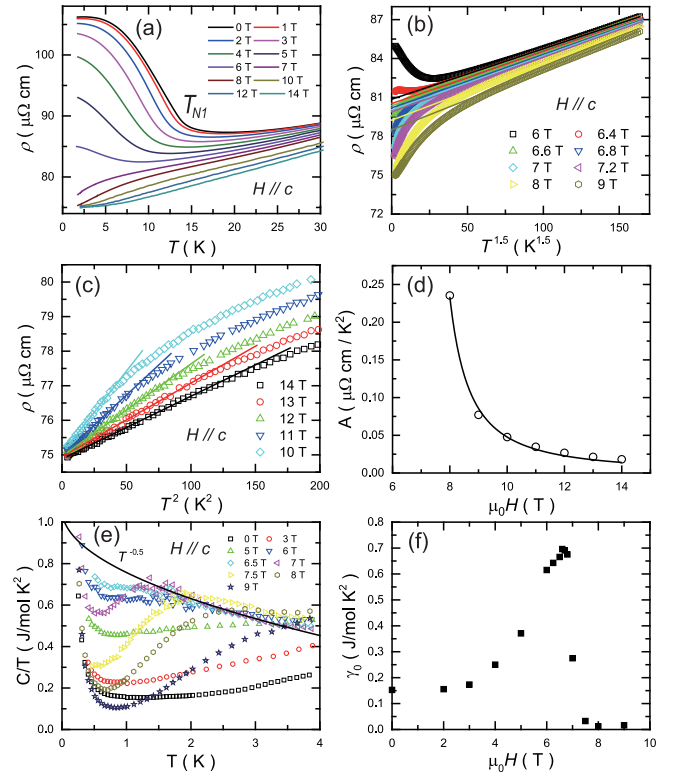


FIG. 4. (a) Temperature dependence of resistivity at different fields. (b) The $T^{1.5}$ dependence of the resistivity around 7 T. The solid lines are fitted by the linear function. (c) The T^2 dependence of the resistivity above 10 T. The solid lines are linear fitting results. (d) The magnetic field dependence of A , which is the coefficient of the T^2 term for the resistivity. The solid line is fitted by $A_0(H - H_{\text{QCP}})^\alpha$. (e) Low-temperature C/T at different fields. The solid line is fitted on the 7-T data by a $T^{-0.5}$ function for $T > 1.5$ K. (f) Magnetic field dependence of γ_0 .

for $H\perp c$, only one can be seen for $H//c$. Moreover, the magnetic susceptibility increases with decreasing temperature below T_{N2} for field vertical to the c axis. These results suggest that the magnetic transition at T_{N2} may involve only the rearrangement of moments within the ab planes. Figures 3(e) and 3(f) plot the M - H loops for field parallel and vertical to the c axis, respectively, which further shows the strong anisotropic behaviors. Clearly, hysteresis is observed at 2 K for $H//c$. This behavior is not associated with conventional ferromagnetism since the hysteresis disappears at zero field, which indicates that it may come from canting of the moments under fields. At 7 T, the moment is about $2.8\mu_B$, which is close to the saturating value of the Nd moment. For $H\perp c$, no hysteresis behavior is found, and the moment at 7 T is still small, which is consistent with the large in-plane Weiss temperature.

Figure 4(a) shows the temperature dependence of the resistivity ρ from 2 to 30 K for $H//c$. At low fields, a sharp upturn appears at T_{N1} , which suggests the opening of a SDW gap. There is no indication of T_{N2} , which is consistent with the magnetic-susceptibility results [Fig. 3(c)]. At 7 T, the upturn disappears, indicating that a SDW QCP may exist. We thus expect that the resistivity ρ should exhibit a power law

behavior around this QCP. Indeed, all the high-temperature data around 7 T show $T^{1.5}$ dependence, as shown in Fig. 4(b), which is consistent with the expectation for a 3D SDW QCP. At low fields, the deviation of $T^{1.5}$ dependence is due to the AFM order. At high fields, the low-temperature resistivity shows typical Fermi-liquid behavior, i.e., $\rho = \rho_0 + AT^2$, as shown in Fig. 4(c). Moreover, the coefficient A shows a divergent behavior with decreasing field [Fig. 4(d)], which is also consistent with the expectation of a QCP. As shown previously [27], one can describe the field dependence of A as $\propto (H - H_{\text{QCP}})^\alpha$, where $H_{\text{QCP}} = 7$ T and α is about -1.5 . Unfortunately, this behavior cannot be traced to 7 T because a $T^{0.5}$ behavior dominates for $T < 2$ K, which will be discussed later.

For a 3D SDW QCP, the low-temperature specific heat C/T does not diverge but shows a $T^{-0.5}$ power law. This is, indeed, the case for our sample near 7 T, as shown in Fig. 4(e). The upturn below 0.5 K is most likely due to the high-temperature tail of the nuclear Schottky anomaly since it shows a T^{-3} temperature dependence [28]. However, the power-law behavior no longer holds for $T \lesssim 1$ K. For fields slightly smaller than 7 T, the C/T for $T < 1$ K is independent of temperature, suggesting the specific heat has a linear temperature dependence, somewhat resembling the Fermi-liquid behavior, although the behavior of the resistivity is not of the Fermi-liquid type. For fields larger than 7 T, a hump appears, and the hump temperature increases with increasing field. Figure 4(f) shows the field dependence of $\gamma_0 = C/T|_{T \rightarrow 0}$ with the nuclear Schottky anomaly removed. Not surprisingly, γ_0 becomes maximum just below 7 T, consistent with the existence of a QCP.

While most of the properties of NdFe_2Ga_8 suggest that there is a 3D SDW QCP around 7 T for $H//c$, the $T^{1.5}$ dependence cannot persist down to zero temperature, as shown in Fig. 4(b). Figure 5(a) shows the temperature dependence of the resistivity at 6.8 T, which follows the $T^{1.5}$ dependence at high temperatures but changes to the $T^{0.5}$ behavior at low temperatures. The square-root temperature dependence of the resistivity does not just show up around the QCP, but rather extends to a large range of magnetic field, from 3 to at least 9 T, as shown in Fig. 5(b).

Before summarizing the results, we provide further analysis of the hysteresis behaviors in the magnetic ordered state below 7 T. As shown in Fig. 3(e), the hysteresis behavior of the magnetic moment can be found for $H//c$. Figure 5(c) shows that the hysteresis can be also found in the difference of the resistivity between increasing and decreasing field processes, i.e., $\Delta\rho_H = \rho_{\text{inc}} - \rho_{\text{dec}}$. Similar to the magnetic hysteresis curves, there is no hysteresis at 0 T, and the maximum is at intermediate fields. It should be noted that at 1.8 K, $\Delta\rho_H$ is not zero above 7 T. Figure 5(d) shows the difference between zero-field-cooled (ZFC) and field-cooled (FC) processes, i.e., $\Delta\rho_T = \rho_{\text{ZFC}} - \rho_{\text{FC}}$, which also shows clear hysteresis behaviors.

Figure 6 gives the phase diagram of NdFe_2Ga_8 for $H//c$ with $\Delta\rho_H/\rho_{\text{inc}}$ in logarithmic scale as the color map. The phase diagram can be divided into five regions, i.e., two AFM ordered regions and the $T^{1.5}$, T^2 , and $T^{0.5}$ regions according to the temperature dependence of the resistivity. The $T^{1.5}$ region exists at high temperatures around 7 T, but it is hard to determine its boundaries precisely because of the large crossover

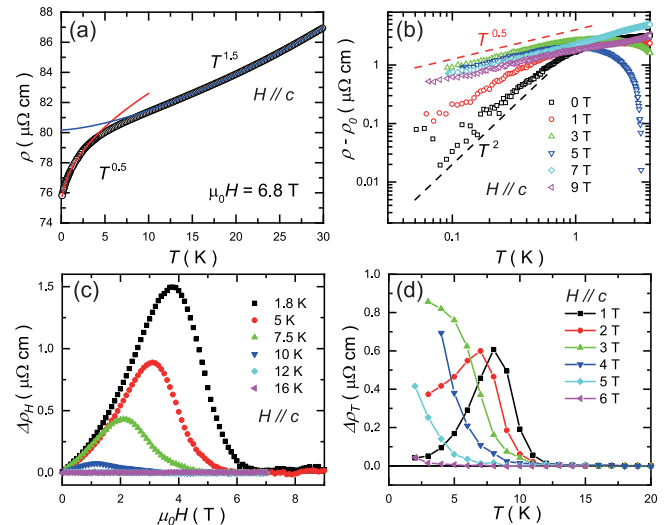


FIG. 5. (a) Temperature dependence of the resistivity at 6.8 T. The solid lines are fitted by the $T^{1.5}$ and $T^{0.5}$ functions. (b) Temperature dependence of $\rho - \rho_0$ at different fields in the log-log scale, where ρ_0 is the extrapolated zero-temperature resistivity. The black and red dashed lines are guides to the T^2 and $T^{0.5}$ dependence, respectively. (c) Field dependence of the resistivity difference between the increasing and decreasing field processes at different temperatures. (d) Temperature dependence of the resistivity difference between the ZFC and FC processes at different fields.

area to either the upturn of the resistivity associated with T_{N1} or the $T^{0.5}$ region at low temperatures. At about 7 T, both T_{N1} and T^+ go to zero. However, they cannot be determined at low temperatures due to the presence of the $T^{0.5}$ dependence of the resistivity, as shown by T^* . Interestingly, the hysteresis area is confined below T_{N2} , rather than T_{N1} , at low fields. Above 4 T when two magnetic transitions are merged, the hysteresis follows the T_{N1} line and seems to end at about 7 T. However, at low temperatures, small but non-negligible hysteresis behavior still persists up to 9 T.

Our results suggest that there are quantum critical fluctuations at about 7 T in NdFe_2Ga_8 , where the AFM order is completely suppressed and Fermi-liquid behavior appears at low temperatures at higher fields, but the hysteresis behaviors in the ordered state may preclude an actual QCP at 0 K. At 7 T, $\rho \sim T^{1.5}$, and $C/T \sim T^{-0.5}$, which is consistent with the theories for the 3D SDW QCPs [1,12]. The $T^{1.5}$ behavior of the resistivity has also been observed in many other itinerant heavy-fermion systems [4–8]. One thing these materials have in common is that they are “dirty”; that is, $\Delta\rho = \rho - \rho_0 \ll \rho_0$ in the temperature range studied. This is also the case for NdFe_2Ga_8 , as shown in Fig. 4(b). Therefore, NdFe_2Ga_8 may be treated as a strong disorder system where the quasiparticles are scattered almost equally strongly over the Fermi surface [1,12]. While the quantum criticality in NdFe_2Ga_8 seems to be conventional, we cannot rule out the possibility of local-moment characteristics for Nd^{3+} . As shown above, the magnetic entropy released at T_{N1} is about $R \ln 2$, which is not expected for a usual SDW AFM order. We thus speculate that the three $4f$ electrons per Nd^{3+} ion exhibit dual behaviors

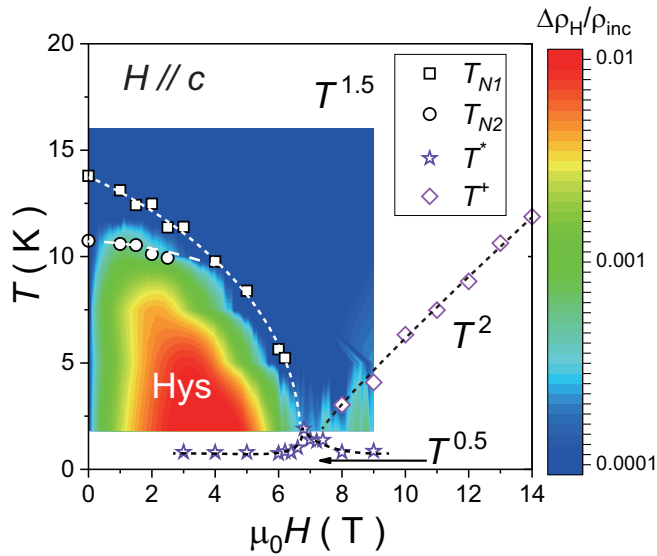


FIG. 6. Phase diagram of NdFe_2Ga_8 for $H//c$. The color map is $\Delta\rho_H/\rho_{\text{inc}}$ in logarithmic scale. T_{N1} and T_{N2} are determined from the resistivity and specific-heat measurements, respectively. Hysteresis behaviors exist in the area below T_{N2} and hence T_{N1} above 4 T, which is labeled as “Hys”, T^+ and T^* represent the characteristic temperatures below which the resistivity follows T^2 and $T^{0.5}$ dependence, respectively. High-temperature resistivity around 7 T shows $T^{1.5}$ dependence. The dashed lines are guides to the eye.

and are partly localized and partly itinerant, both of which contribute to the AFM order.

It should be pointed out that although we have assumed that both magnetic transitions in NdFe_2Ga_8 are from the AFM orders, further studies are needed to reveal their nature. Particularly, we would like to emphasize the hysteresis behavior below T_{N2} is not from the FM ordering, although the Weiss temperature for $H//c$ is positive. As shown in both the magnetic-susceptibility and resistivity data [Figs. 3(e) and 5(c)], there is no difference for the field-increasing and field-decreasing processes at zero field, which is not the case for a FM order. It seems that the FM moment appears only under field, which indicates that it may be related to the field-induced canting moments, but how to understand the hysteresis remains unclear.

Another mystery in the NdFe_2Ga_8 system is why the temperature dependence of the resistivity is $T^{0.5}$ at low temperatures. In some disordered systems close to the metal-insulator transition, similar behaviors have been found [29,30]. As discussed above, NdFe_2Ga_8 is, indeed, a dirty system, which seems to explain the $T^{0.5}$ dependence. How-

ever, no such behavior has been found in other dirty itinerant heavy-fermion systems [4–8]. Moreover, the low-temperature resistivity at zero field actually shows T^2 dependence as a Fermi liquid, as shown in Fig. 4(b). $T^{0.5}$ appears only when the magnetic field is large enough. We thus suspect that it is the FM component associated with the hysteresis behavior that results in the low-temperature $T^{0.5}$ dependence of the resistivity. The FM fluctuations have been shown to be able to affect the resistivity [31,32]. In our case, the FM moment is induced by the magnetic field and shows 1D characteristics, which explains why $T^{0.5}$ appears only under sufficiently large magnetic field. It is interesting to note that T^* in Fig. 6 is largest at 6.8 T, where the long-range AFM order disappears, which seems to suggest that the FM fluctuations may be coupled to the AFM critical fluctuations. Thus, we cannot exclude the possibility of a failed quantum critical point interrupted by these effects. It should also be noted that we have neglected the Fe moments in the above discussions, which may also contribute to the very low temperature magnetic properties.

IV. CONCLUSIONS

Our systematic results suggest there may be a magnetic QCP in the NdFe_2Ga_8 system when the AFM order is completely suppressed by a 7-T magnetic field parallel to the c axis. The quantum criticality show clear signs for a 3D SDW type of QCP, including $\rho \sim T^{1.5}$ and $C/T \sim T^{-0.5}$. However, the resistivity shows $T^{0.5}$ dependence at very low temperatures for field larger than 3 T, which may be attributed to the field-induced FM moment and may result in a failed QCP. It is interesting to note that a coupling between the FM fluctuations and the AFM quantum critical fluctuations may exist at 7 T. More detailed studies are needed to further understand the electronic and spin systems of NdFe_2Ga_8 .

ACKNOWLEDGMENTS

This work is supported by the National Key R&D Program of China (Grants No. 2017YFA0302900, No. 2017YFA0303103, No. 2016YFA0300502, No. 2016YFA0300604), the National Natural Science Foundation of China (Grants No. 11874401, No. 11674406, No. 11961160699, No. 11774399), the Strategic Priority Research Program of the Chinese Academy of Sciences (Grant No. XDB33010000), the Beijing Natural Science Foundation (Grant No. Z180008), the K. C. Wong Education Foundation (Grant No. GJTD-2018-01), and the Fund of Science and Technology on Surface Physics and Chemistry Laboratory (201901SY00900102).

C.W. and X.W. contributed equally to this work.

- [1] H. v. Löhneysen, A. Rosch, M. Vojta, and P. Wölfle, *Rev. Mod. Phys.* **79**, 1015 (2007).
- [2] O. Stockert and F. Steglich, *Annu. Rev. Condens. Matter Phys.* **2**, 79 (2011).
- [3] P. Gegenwart, F. Steglich, C. Geibel, and M. Brando, *Eur. Phys. J.: Spec. Top.* **224**, 975 (2015).

- [4] S. R. Julian, C. Pfleiderer, F. M. Grosche, N. D. Mathur, G. J. McMullan, A. J. Diver, I. R. Walker, and G. G. Lonzarich, *J. Phys.: Condens. Matter* **8**, 9675 (1996).
- [5] P. Gegenwart, C. Langhammer, C. Geibel, R. Helfrich, M. Lang, G. Sparn, F. Steglich, R. Horn, L. Donnevert, A. Link, and W. Assmus, *Phys. Rev. Lett.* **81**, 1501 (1998).

- [6] R. Hauser, M. Galli, E. Bauer, A. Kottar, G. Hilscher, and D. Kaczorowski, *J. Magn. Magn. Mater.* **177–181**, 292 (1998).
- [7] K. Heuser, E.-W. Scheidt, T. Schreiner, and G. R. Stewart, *Phys. Rev. B* **58**, R15959(R) (1998).
- [8] F. M. Grosche, P. Agarwal, S. R. Julian, N. J. Wilson, R. K. W. Haselwimmer, S. J. S. Lister, N. D. Mathur, F. V. Carter, S. S. Saxena, and G. G. Lonzarich, *J. Phys.: Condens. Matter* **12**, L533 (2000).
- [9] H. Q. Yuan, F. M. Grosche, M. Deppe, G. Sparn, C. Geibel, and F. Steglich, *Phys. Rev. Lett.* **96**, 047008 (2006).
- [10] J. Arndt, O. Stockert, K. Schmalzl, E. Faulhaber, H. S. Jeevan, C. Geibel, W. Schmidt, M. Loewenhaupt, and F. Steglich, *Phys. Rev. Lett.* **106**, 246401 (2011).
- [11] Y. Matsumoto, M. Sugi, N. Kimura, T. Komatsubara, H. Aoki, I. Satoh, T. Terashima, and S. Uji, *J. Phys. Soc. Jpn.* **77**, 053703 (2008).
- [12] T. Moriya and T. Takimoto, *J. Phys. Soc. Jpn.* **64**, 960 (1995).
- [13] O. M. Sichevich, R. V. Lapunova, Y. Grin, and Y. P. Yarmolyuk, *Izv. AN SSSR. Metall* **6**, 109 (1985).
- [14] M. Kolenda, M. D. Koterlin, M. Hofmann, B. Penc, A. Szytula, A. Zygmunt, and J. Żukrowski, *J. Alloys Compd.* **327**, 21 (2001).
- [15] S. Ghosh and A. M. Strydom, *Acta Phys. Pol. A* **121**, 1082 (2012).
- [16] K. Cheng, L. Wang, Y. Xu, F. Yang, H. Zhu, J. Ke, X. Lu, Z. Xia, J. Wang, Y. Shi, Y. Yang, and Y. Luo, *Phys. Rev. Mater.* **3**, 021402 (2019).
- [17] A. Tursina, E. Khamitcaeva, D. Gnida, and D. Kaczorowski, *J. Alloys Compd.* **731**, 229 (2018).
- [18] L. Wang, Z. Fu, J. Sun, M. Liu, W. Yi, C. Yi, Y. Luo, Y. Dai, G. Liu, Y. Matsushita, K. Yamaura, L. Lu, J.-G. Cheng, Y. Yang, Y. Shi, and J. Luo, *npj Quantum Mater.* **2**, 36 (2017).
- [19] A. Bhattacharyya, D. T. Adroja, J. S. Lord, L. Wang, Y. Shi, K. Panda, H. Luo, and A. M. Strydom, *Phys. Rev. B* **101**, 214437 (2020).
- [20] M. Schlüter and W. Jeitschko, *Inorg. Chem.* **40**, 6362 (2001).
- [21] O. Tougait, D. Kaczorowski, and H. Noël, *J. Solid State Chem.* **178**, 3639 (2005).
- [22] H. S. Nair, S. K. Ghosh, K. R. Kumar, and A. M. Strydom, *J. Phys. Chem. Solids* **91**, 69 (2016).
- [23] M. O. Ogunbunmi, B. M. Sondezi, H. S. Nair, and A. M. Strydom, *Phys. B (Amsterdam, Neth.)* **536**, 128 (2018).
- [24] M. O. Ogunbunmi, H. S. Nair, and A. M. Strydom, *JPS Conf. Proc.* **30**, 011114 (2020).
- [25] P. Watkins-Curry, J. V. Burnett, T. Samanta, D. P. Young, S. Stadler, and J. Y. Chan, *Cryst. Growth Des.* **15**, 3293 (2015).
- [26] M. O. Ogunbunmi, *Prog. Solid State Chem.* **58**, 100275 (2020).
- [27] J. Paglione, M. A. Tanatar, D. G. Hawthorn, E. Boaknin, R. W. Hill, F. Ronning, M. Sutherland, L. Taillefer, C. Petrovic, and P. C. Canfield, *Phys. Rev. Lett.* **91**, 246405 (2003).
- [28] R. Küchler, N. Oeschler, P. Gegenwart, T. Cichorek, K. Neumaier, O. Tegus, C. Geibel, J. A. Mydosh, F. Steglich, L. Zhu, and Q. Si, *Phys. Rev. Lett.* **91**, 066405 (2003).
- [29] P. Dai, Y. Zhang, and M. P. Sarachik, *Phys. Rev. B* **45**, 3984 (1992).
- [30] S. Žonja, M. Očko, M. Ivanda, and P. Biljanović, *J. Phys. D* **41**, 162002 (2008).
- [31] T. Moriya, *J. Magn. Magn. Mater.* **14**, 1 (1979).
- [32] M. Kataoka, *Phys. Rev. B* **63**, 134435 (2001).